

Site-specific differential effects of once-yearly zoledronic acid on the hip assessed with quantitative computed tomography: results from the HORIZON Pivotal Fracture Trial

L. Yang · A. V. Sycheva · D. M. Black · R. Eastell

Received: 5 December 2011 / Accepted: 29 August 2012 / Published online: 6 November 2012
© International Osteoporosis Foundation and National Osteoporosis Foundation 2012

Abstract

Summary We used new approaches to the analysis of diagnostic scans to detect changes in bone density in different regions of the hip after 3 years of treatment with the zoledronic acid. We showed that the drug significantly increases hip bone density compared to placebo at regions where hip fractures usually occur.

Introduction This study aims to identify whether treatment with zoledronic acid exerts site-specific differential effects on volumetric bone mineral density (vBMD) at the hip.

Methods We analysed quantitative computed tomography scans of the hip obtained at baseline and 36 months in 179 women participating in the HORIZON Pivotal Fracture Trial. Cortical, trabecular and integral BMDs were determined at three main regions of interest—the femoral neck (FN), trochanter (TR) and total hip (TH)—and several sub-regions of interest, namely the proximal, middle, distal, anterior, posterior, inferomedial and superolateral FN, and the middle and distal TR.

Results Volumetric BMD increased significantly ($p < 0.05$) from baseline with zoledronic acid compared to placebo. Trabecular vBMD increased as follows: FN, 5.4 %; FN sub-regions, 6.0 % (proximal), 4.4 % (middle), 5.6 % (distal), 7.5 % (anterior), 7.0 % (superolateral) and 5.4 % (posterior); TR, 6.5 % and TH, 5.7 %. Cortical vBMD increased as follows: FN sub-regions, 5.0 % (proximal FN) and 2.3 % (anterior); TR, 4.6 %; middle TR, 2.7 % and TH, 3.8 %.

Conclusions The effects on vBMD of annual infusion of 5 mg of zoledronic acid are site-specific and dominated by trabecular changes.

Keywords Bisphosphonates · Bone QCT · Osteoporosis · Volumetric BMD · Zoledronic acid

Introduction

Age-associated reduction in bone density of the femur is site-specific, with relative preservation of the inferior region of the femoral neck (FN) and greatly reduced cortical thickness and trabecular volumetric BMD (vBMD) at the superolateral aspect of the FN in elderly compared to young women [1–3]. These changes have important implications as hip fracture is often initiated by a local failure at the superolateral aspect of the FN during a sideways fall [4]. Both cortical and trabecular bone contribute to femoral strength [5–8] and resistance to cortical buckling [3, 9], but we might expect to see a greater response to anti-resorptive therapy in trabecular bone due to its higher bone turnover. This could result in different site (region)-specific treatment effects since the trabecular bone is heterogeneously distributed in the proximal femur [1, 2, 10, 11]. Several clinical studies have reported an increased hip vBMD following anti-resorptive therapy [12–17], whereas only one

L. Yang · A. V. Sycheva · R. Eastell
Academic Unit of Bone Metabolism, University of Sheffield,
Sheffield S10 2RX, UK

A. V. Sycheva
e-mail: anyasycheva03@googlemail.com

R. Eastell
e-mail: r.eastell@sheffield.ac.uk

D. M. Black
Department of Epidemiology and Biostatistics,
University of California,
San Francisco, CA, USA
e-mail: DBlack@psg.ucsf.edu

L. Yang (✉)
School of Medicine and Biomedical Sciences, Beech Hill Road,
Sheffield S10 2RX, UK
e-mail: l.yang@sheffield.ac.uk

examined site-specific response to parathyroid hormone (1–34) [18].

In this study, we investigated the effects of zoledronic acid on the cortical and trabecular compartments of different regions of the proximal femur using quantitative computed tomography (QCT)-based three-dimensional hip structural analysis. The Horizon QCT study has already been published [14], but the analysis reported here was designed to address different questions. We hypothesised that treatment with zoledronic acid would result in changes in cortical and trabecular bone that vary in different regions of the hip. These effects may help to explain the reduction in risk of hip fracture in patients treated with zoledronic acid.

Materials and methods

Study participants

In the HORIZON Pivotal Fracture Trial (HORIZON PFT), 3,889 postmenopausal women were randomly assigned to receive a single 15-min infusion of zoledronic acid (Novartis Pharma, Basel, Switzerland) at baseline, 12 and 24 months, and 3,876 were assigned to receive a matching placebo. Patients were followed for 36 months from baseline. A pre-planned QCT study was performed in a subset of the full study population ($n=233$). Two hundred thirty-two patients had hip QCT scans at baseline and 181 patients had hip QCT scans at year 3 (two of the patient scans performed at year 3 were lost). We analysed 179 scans that were available at both baseline and year 3 (94 in the zoledronic acid group and 85 in the placebo group). Table 1 shows the baseline patient characteristics.

The HORIZON PFT was conducted in compliance with the ethical principles of the Declaration of Helsinki (1989) and local applicable laws and regulations. Approval was obtained from an Institutional Review Board, Independent Ethics Committee or Research Ethics Board by each participating centre. Patients provided written informed consent to participate in the study.

Quantitative computed tomography

The QCT scans were acquired as described previously [14]. Patients were positioned supine with a density calibration phantom (Image Analysis, Columbia KY, USA) placed beneath the hips. The superior limit of the scan was 5 mm above the acetabulum and the inferior limit was 5 mm below the lesser trochanter. Scan parameters were 3-mm section thickness (pitch=1), 80 kVp and 280 mAs, standard reconstruction kernel, with an in-plane pixel size of 0.94–0.97 mm and slice thickness of 3.0 mm. The CT images were archived to DICOM CD-ROM for further analysis. For

quality control, a calibration phantom (Image Analysis) was scanned every 2 weeks during the study period. A cross-centre calibration scan was also performed using the same Image Analysis calibration phantom at all clinical centres.

Three-dimensional hip structural analysis

Analysis was performed blinded to treatment status. Programs were developed using Matlab (The Mathworks Inc., Natick, MA, USA) for the analysis of QCT scans; this has been described previously [10]. Only the left hip was analysed. The Hounsfield unit of each voxel was converted to mineral density using the density calibration phantom. The outer contours of the proximal femur were determined slice by slice by using an interactive program that combines density-thresholding at 100 mg/cm³, morphological operation and manual tracing. From this point onwards, image processing and calculations were performed automatically. The scans were re-sampled using linear interpolation so that the voxel size was 1×1×1 mm³. The femora was digitally rotated to a standard orientation to compensate for variation in patient positioning during scanning (Fig. 1). We measured cortical, trabecular and integral vBMD in a series of cross-sectional regions and sub-regions of interest along the axes of the neck and shaft of the femur (Fig. 1). We identified three main regions of interest, namely the FN, trochanter (TR) and total hip (TH) (FN plus TR). The sub-regions of the FN were three cross-sectional sections, namely the proximal, middle and distal FN, and four quadrants (with the origin at the geometrical centre of the FN cross sections), namely the anterior, posterior, inferomedial and superolateral FN. Two cross-sectional sub-regions were also identified in the TR, namely the middle and the distal TR. Volumetric BMDs in the main and sub-regions of interest were calculated by averaging voxel vBMD over the relevant volumes.

To define cortical bone, we developed and validated a method for analysis of QCT hip scans with an in-plane pixel resolution of about 1 mm. This method has been described and validated [19]. The images were enlarged by four times using bilinear interpolation so that the pixel size was about 0.25 by 0.25 mm. For each cross section, density profiles perpendicular to the periosteal surface (segmented by thresholding already) were generated at every other periosteal surface pixels and the periosteal border k_p in the profile was identified. The maximum density D_{max} and the middle location k_{max} of $0.85D_{max}$ in the profiles were identified. If $D_{max} < 0.2D_{FN}$ (D_{FN} , maximum density of the whole FN), which indicates a thin cortex, k_{max} is checked: if $k_p - k_{max} > 2.5$ mm, k_{max} is adjusted so that $k_p - k_{max} = 1.25$ mm. The endosteal border k_e is defined as the mirror point of k_p with respect to k_{max} , i.e., doubling the width of $k_p - k_{max}$. A five-point moving average filter was used to smooth the endosteal border points k_e in a cross section and the resulting

Table 1 Baseline patient characteristics and DXA and QCT measurements

Patient characteristics	Zoledronic acid		HORIZON PFT		Placebo		HORIZON PFT	
	This study	Eastell et al. [14]	This study	Eastell et al. [14]	This study	Eastell et al. [14]	This study	Eastell et al. [14]
Zoledronic acid								
Number	94	122	3875	3875	85	111	3861	3861
Age (year)	73.1 (5.2)	74.2 (5.6)	73.1 (5.3)	73.1 (5.3)	73.4 (6.2)	74.3 (6.4)	73.0 (5.4)	73.0 (5.4)
Height (cm)	152.9 (6.7)	152.1 (6.7)	154.4 (7.1)	154.4 (7.1)	154.0 (6.2)	153.7 (6.3)	154.4 (7.0)	154.4 (7.0)
Weight (kg)	58.9 (10.8)	58.0 (11.2)	59.9 (11.1)	59.9 (11.1)	59.7 (11.2)	58.9 (11.4)	60.6 (11.3)	60.6 (11.3)
BMI (kg/m ²)	25.2 (4.1)	25.0 (4.3)	25.1 (4.3)	25.1 (4.3)	25.1 (3.9)	24.8 (3.9)	25.4 (4.3)	25.4 (4.3)
aBMD (g/cm ²)								
Number	94	122	3,844-3,851	3,844-3,851	84	110	3,839-3,845	3,839-3,845
FN aBMD	0.568 (0.081)	0.562 (0.080)	0.580 (0.086)	0.580 (0.086)	0.558 (0.083)	0.547 (0.088)	0.581 (0.089)	0.581 (0.089)
TR aBMD	0.525 (0.092)	0.515 (0.090)	0.518 (0.094)	0.518 (0.094)	0.512 (0.097)	0.502 (0.102)	0.518 (0.095)	0.518 (0.095)
TH aBMD	0.683 (0.101)	0.673 (0.097)	0.668 (0.093)	0.668 (0.093)	0.669 (0.098)	0.652 (0.106)	0.669 (0.094)	0.669 (0.094)
	Zoledronic acid (n=94)				Placebo (n=85)			
	Cortical	Trabecular	Integral	Integral	Cortical	Trabecular	Integral	Integral
vBMD (g/cm³)								
Total FN	0.431 (0.064)	0.143 (0.031)*	0.230 (0.042)	0.230 (0.042)	0.431 (0.055)	0.133 (0.033)*	0.225 (0.040)	0.225 (0.040)
Total TR	0.414 (0.055)*	0.102 (0.024)*	0.191 (0.032)*	0.191 (0.032)*	0.397 (0.068)*	0.096 (0.024)*	0.182 (0.035)*	0.182 (0.035)*
TH	0.422 (0.060)	0.122 (0.028)	0.210 (0.037)	0.210 (0.037)	0.414 (0.062)	0.115 (0.029)	0.204 (0.038)	0.204 (0.038)
Proximal FN	0.257 (0.057)	0.189 (0.049)	0.223 (0.053)	0.223 (0.053)	0.262 (0.053)	0.177 (0.048)	0.220 (0.050)	0.220 (0.050)
Middle FN	0.366 (0.065)	0.165 (0.040)	0.266 (0.054)	0.266 (0.054)	0.370 (0.060)	0.154 (0.037)	0.262 (0.050)	0.262 (0.050)
Distal FN	0.406 (0.059)	0.150 (0.037)	0.278 (0.049)	0.278 (0.049)	0.402 (0.062)	0.146 (0.036)	0.274 (0.051)	0.274 (0.051)
Middle TR	0.387 (0.055)	0.122 (0.035)	0.255 (0.046)	0.255 (0.046)	0.371 (0.059)	0.116 (0.035)	0.244 (0.049)	0.244 (0.049)
Distal TR	0.764 (0.065)*	0.119 (0.018)*	0.465 (0.075)	0.465 (0.075)	0.744 (0.074)*	0.125 (0.018)*	0.456 (0.082)	0.456 (0.082)
Inferomedial FN	0.580 (0.090)	0.267 (0.035)*	0.424 (0.048)	0.424 (0.048)	0.592 (0.074)	0.259 (0.034)*	0.426 (0.041)	0.426 (0.041)
Anterior FN	0.261 (0.043)	0.133 (0.038)*	0.197 (0.029)	0.197 (0.029)	0.262 (0.045)	0.124 (0.036)*	0.193 (0.029)	0.193 (0.029)
Superolateral FN	0.222 (0.037)	0.117 (0.038)*	0.169 (0.027)*	0.169 (0.027)*	0.215 (0.039)	0.107 (0.040)*	0.161 (0.028)*	0.161 (0.028)*
Posterior FN	0.323 (0.044)	0.156 (0.040)	0.240 (0.030)	0.240 (0.030)	0.324 (0.053)	0.148 (0.035)	0.236 (0.032)	0.236 (0.032)
Volume (cm³)								
Total FN	3.43 (0.93)	8.00 (2.15)	11.42 (2.98)	11.42 (2.98)	3.58 (0.81)	8.13 (1.91)	11.70 (2.64)	11.70 (2.64)
Total TR	13.46 (2.04)	34.26 (6.72)	47.72 (8.53)	47.72 (8.53)	14.00 (1.97)	35.26 (5.72)	49.26 (7.34)	49.26 (7.34)
TH	16.88 (2.24)*	42.26 (7.06)	59.15 (9.03)*	59.15 (9.03)*	17.58 (2.13)*	43.39 (6.04)	60.96 (7.80)*	60.96 (7.80)*
Proximal FN	1.28 (0.12)*	3.49 (0.12)*	4.77 (0.13)*	4.77 (0.13)*	1.35 (0.10)*	3.66 (0.10)*	5.01 (0.12)*	5.01 (0.12)*
Middle FN	1.31 (0.09)	2.99 (0.09)	4.29 (0.16)	4.29 (0.16)	1.32 (0.08)	2.96 (0.08)	4.28 (0.13)	4.28 (0.13)
Distal FN	1.46 (0.10)*	3.28 (0.10)*	4.47 (0.23)*	4.47 (0.23)*	1.54 (0.09)*	3.40 (0.09)*	4.94 (0.17)*	4.94 (0.17)*
Middle TR	1.58 (0.12)	5.82 (0.11)	7.40 (0.11)	7.40 (0.11)	1.58 (0.12)	5.83 (0.11)	7.41 (0.10)	7.41 (0.10)
Distal TR	1.58 (0.12)	3.52 (0.13)*	5.10 (0.13)*	5.10 (0.13)*	1.58 (0.11)	*3.58 (0.12)	5.16 (0.12)*	5.16 (0.12)*

Table 1 (continued)

Inferomedial FN	1.28 (0.44)	2.54 (0.76)	3.82 (0.44)	1.32 (0.34)	2.60 (0.66)	3.92 (0.37)
Anterior FN	0.87 (0.22)	2.20 (0.61)	3.07 (0.32)	0.91 (0.18)	2.25 (0.50)	3.16 (0.27)
Superolateral FN	0.99 (0.27)	2.79 (0.87)	3.78 (0.46)*	1.03 (0.32)	2.89 (0.75)	3.92 (0.39)*
Posterior FN	0.90 (0.23)	2.22 (0.60)	3.12 (0.32)*	0.94 (0.18)	2.29 (0.52)	3.23 (0.28)*

The results are presented as mean (standard deviation)

* $p < 0.05$ (significant difference between the zoledronic acid and placebo groups)

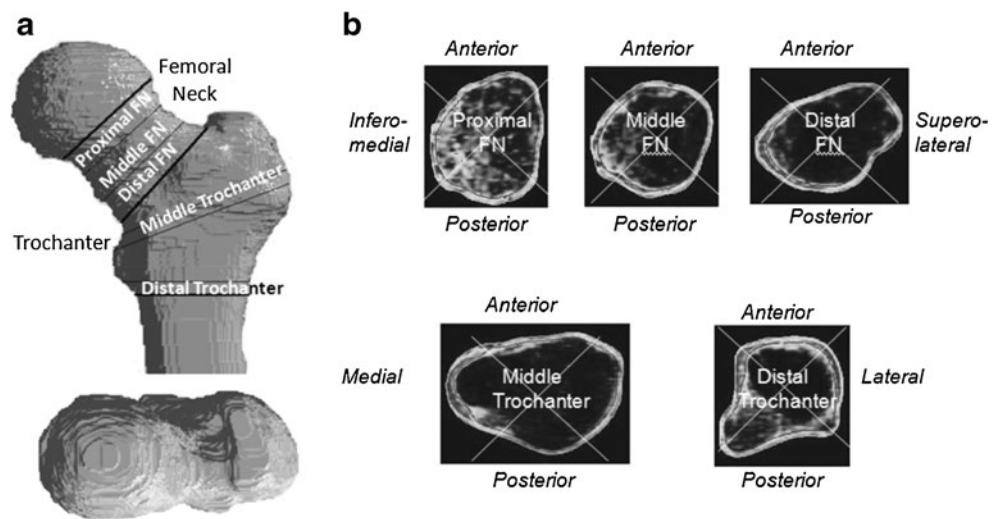
points were connected to form a continuous endosteal border. We further validated the method in an ex vivo analysis of the human FN ($n=3$) scanned by a micro CT (μ CT 100, SCANCO Medical AG, Brüttisellen, Switzerland) at a resolution of 0.062 mm. We analysed 11 evenly distributed slices between the subcapital and distal FN from each of the three specimens and segmented the cortical region by threshold and manual tracing. We simulated QCT scans of 1.0-mm pixel size by averaging the original micro CT images in 16×16 pixel blocks and applied our method for cortical segmentation (Fig. 2). We did not perform QCT on these samples because this might have introduced variation due to differences in positioning or in defining the regions of interest. We compared cortical, trabecular and integral area, vBMD and cortical thickness in the anterior, posterior, inferomedial and superolateral FN quadrants calculated by both micro CT and simulated QCT (Table 2). With micro CT as the standard, our method (1) underestimated the cortical area by 6 % in the inferomedial quadrant (where the cortex is relatively thick) and overestimated the cortical area by 7–16 % in the superolateral and posterior quadrants (where the cortex is relatively thin). On average, cortical area of the posterior and superolateral quadrants of the FN in this validation study was 27 mm^2 and a 16 % error in the area accounts for only 4.3 pixels in the simulated clinical CT. (2) Our method underestimated cortical vBMD by 12 % in the inferomedial quadrant and by 31–34 % in the other quadrants, which was expected since measurement of vBMD decreases with reduced QCT resolution and cortical thickness by as much as 60 % [20, 21]. (3) Our method overestimated trabecular vBMD and underestimated integral vBMD by 3–5 %.

We assessed the intra-observer reproducibility of 3-D hip structure analysis by analysing 16 randomly selected 36-month scans on three separate occasions, 1 week apart. The coefficient of variation (CV) ranged from 0.5 to 2.6 % for measurement of vBMD (Table 3).

Statistical analysis

Statistical analysis of the data was carried out at the University of California, San Francisco (Department of Epidemiology and Biostatistics). We used the two-sample t test to compare mean age, height, weight, body mass index (BMI), areal BMD (aBMD) and vBMD at baseline and 36 months between the zoledronic acid and placebo groups. For each patient, we calculated percentage changes from baseline of the variables and the group mean and 95 % confidence intervals (CI) of the percentage change in aBMD and vBMD. These values were then used to assess the significance of the between-treatment differences using the two-sample t test. We used a threshold of $p < 0.05$ to denote statistical significance.

Fig. 1 **a** Standard orientation of the femur and definitions of various regions of interest in the study. Cross sections were defined in the whole femoral neck and middle and distal TR. **b** Typical cross sections in the subcapital, middle and basal capsule of the FN and middle and distal TR with inferomedial, anterior, superolateral and posterior quadrants



Results

Baseline characteristics

Mean age, weight, height and BMI were similar in the zoledronic acid and placebo groups (Table 1), so were the FN, TR and TH aBMDs; the means were also similar to those in the full subset of 233 patients who underwent QCT [14] and to the whole HORIZON PFT population [22]. There were some differences in baseline QCT measures: higher mean vBMD at the FN and TR (but not TH) in the zoledronic acid compared to the placebo group, larger volumes in proximal and distal FN and TH in placebo group (Table 1).

Changes from baseline in aBMD at 36 months

Table 4 lists the FN, TR and TH aBMDs at baseline and at 36 months. Compared with baseline value, aBMD

increased in the zoledronic acid group (only significantly at TR, $p < 0.05$) and remained almost constant in the placebo group. Compared with placebo, there were 5.3, 7.6 and 5.3 % increases ($p < 0.0001$) in the FN, TR and TH aBMDs, respectively. These values were similar to those obtained from the whole QCT (5.1, 7.4 and 5.1 %) and HORIZON PFT cohorts (5.0, 8.2 and 6.0 %).

Changes from baseline in volume at 36 months

Table 5 shows the percentage change from baseline in volumes of various regions of interests. The percentage changes ranged from -1.8 % for trabecular volume at middle TR to 6.2 % for cortical volume at the anterior quadrant of the FN. These small values are an indication that segmentation of various regions was consistent.

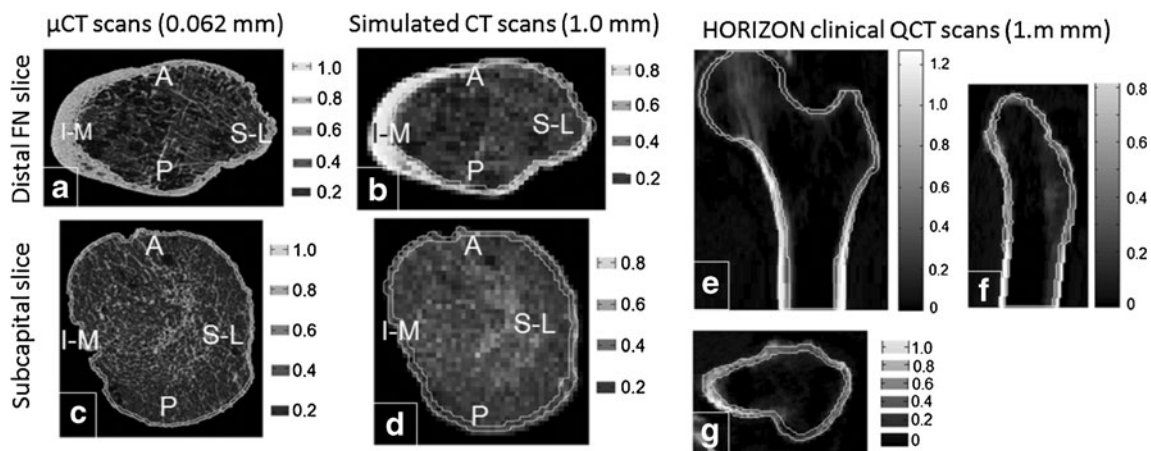


Fig. 2 Typical micro CT images of the **a** distal femoral neck and **c** subcapital and the corresponding simulated clinical QCT images (**b**) and (**d**). Note the similarity in cortical region between the micro CT and simulated clinical QCT. *I-M*, inferior-medial; *S-P*, superior-lateral;

A, anterior; *P*, posterior. Images **e** to **g** shows the frontal, sagittal and sagittal plane QCT slices of a typical study patient showing cortical segmentation

Table 2 Mean (95 % CI) percentage error of QCT measurements from the simulated QCT in comparison with micro CT

	Area			vBMD		
	Cortical	Trabecular	Integral	Cortical	Trabecular	Integral
Inferomedial	-6 (-13, 0)	2 (1, 4)	-1 (-1, 0)	-12 (-15, -9)	6 (4, 8)	-3 (-3, -3)
Anterior	7 (-1, 15)	-1 (-2, 0)	-1 (-1, -1)	-31 (-34, -29)	4 (3, 5)	-5 (-6, -5)
Superolateral	16 (7, 26)	-2 (-3, -2)	-1 (-1, -1)	-33 (-35, -31)	3 (2, 4)	-5 (-5, -5)
Posterior	15 (4, 26)	-1 (-2, -1)	-1 (-1, 0)	-34 (-36, -32)	5 (3, 6)	-5 (-6, -5)
Total image	4 (-3, 11)	2 (1, 2)	1 (1, 2)	-24 (-26, -22)	5 (4, 6)	-3 (-3, -3)

Changes from baseline in vBMD at 36 months

Figure 3 shows the percent changes from baseline in vBMD in the zoledronic acid and placebo groups and the differences between groups in the change measured at 36 months. In the zoledronic acid group, trabecular and integral vBMD increased significantly across the main regions of interest (at FN $p < 0.05$ trabecular only, at TR $p < 0.001$ and at TH $p < 0.01$). The trabecular increases were significant ($p < 0.05$) across all of the sub-regions except the middle and superolateral FN, whereas the increase in integral vBMD was significant ($p < 0.05$) at the superolateral FN only. Cortical vBMD increased significantly at the TR only ($p < 0.05$), but on sub-regional analysis, there was a significant ($p < 0.001$) increase at the superolateral FN. There were also significant decreases in sub-regional cortical vBMD at the distal ($p < 0.05$) and posterior ($p < 0.001$) FN in the zoledronic acid group.

In the placebo group, vBMD decreased significantly across the FN, TR and TH ($p < 0.01$) and several sub-regions ($p < 0.05$); the exceptions were the middle (trabecular and integral), distal (trabecular and integral), inferomedial (trabecular) and posterior (trabecular) regions of the FN,

superolateral FN (cortical vBMD) and the distal TR (trabecular and integral vBMD).

The between-treatment differences in vBMD were all significant in all main regions (FN, TR and TH) in favour of the zoledronic acid ($p < 0.01$) with the exception of cortical vBMD at FN. The differences in trabecular and integral vBMD were also significant ($p < 0.05$) across most of the sub-regions, with the exception of integral vBMD at the middle, distal and inferomedial FN and the distal TR, and trabecular vBMD at inferomedial FN. The difference between groups in cortical vBMD was significant at the proximal and anterior FN and the middle TR. Although not statistically significant ($p > 0.05$), the differences in trabecular vBMD were higher than the differences in cortical vBMD for all but one region. It was interesting to note that the differences in integral vBMD of the FN, TR and TH (3.9, 6.0 and 5.6 %, respectively) were similar to the corresponding aBMD (5.3, 7.6 and 5.3 %, respectively).

Discussion

There is recent evidence that ongoing loss in cortical and trabecular bone is concentrated at the superolateral aspect of the FN [1–3] and that cortical bone reduction resulting from cortical thinning and increased porosity at the anterior and inferoanterior regions is associated with FN fractures [23–25]. Volumetric BMD does increase with anti-resorptive therapy, but there is little evidence about site-specific responses. In this clinical study, we determined the effects of zoledronic acid on the cortical and trabecular compartments of different partitions of the proximal femur. The decreases in vBMD observed over 3 years in the placebo group reflect age-related bone loss. In contrast, there were significant increases from baseline in vBMD with zoledronic acid. The increases in trabecular vBMD across the different sub-regions were more consistent than for cortical or integral vBMD. Our between-treatment results suggest that in comparison with the placebo, zoledronic acid significantly increases bone density, particularly in trabecular compartment and in the sub-regions of the hip that have been associated with the initiation of hip fracture.

Table 3 Intra-observer reproducibility of vBMD (percentage of CV)

	Cortical	Trabecular	Integral
FN			
Proximal	2.6	1.4	2.0
Middle	1.5	2.0	1.5
Distal	1.3	2.0	1.4
Inferomedial	2.0	1.5	1.8
Anterior	0.9	1.6	0.9
Superolateral	0.8	2.4	1.0
Posterior	2.0	2.6	2.1
Total	1.2	1.2	1.2
TR			
Middle	1.6	1.7	1.0
Distal	1.3	0.9	0.9
Total	0.8	1.2	0.9
TH	0.7	0.5	0.6

Table 4 Mean (SD) areal BMD (in grams per square centimetre) at baseline and year 3 and percent change from baseline

	Zoledronic Acid			Placebo		
	This study	Eastell et al. [14]	HORIZON PFT	This study	Eastell et al. [14]	HORIZON PFT
Baseline						
Number	94	122	3,844–3,851	84	110	3,839–3,845
FN aBMD	0.568 (0.081)	0.562 (0.080)	0.580 (0.086)	0.558 (0.083)	0.547 (0.088)	0.581 (0.089)
TR aBMD	0.525 (0.092)	0.515 (0.090)	0.518 (0.094)	0.512 (0.097)	0.502 (0.102)	0.518 (0.095)
TH aBMD	0.683 (0.101)	0.673 (0.097)	0.668 (0.093)	0.669 (0.098)	0.652 (0.106)	0.669 (0.094)
Year 3						
Number	93	97	3,076–3,082	84	86	3,086–3,092
FN aBMD	0.591 (0.086)	0.587 (0.087)	0.604 (0.091)	0.554 (0.085)	0.554 (0.084)	0.578 (0.090)
TR aBMD	0.557 (0.100)	0.552 (0.101)	0.556 (0.097)	0.507 (0.102)	0.508 (0.102)	0.516 (0.098)
TH aBMD	0.708 (0.106)	0.704 (0.107)	0.700 (0.095)	0.660 (0.103)	0.662 (0.102)	0.663 (0.097)
% change						
Number	93	97	3,061–3067	84	86	3,077–3,083
FN aBMD	4.2 (6.1)	4.0 (6.1)	4.1 (5.8)	−1.1 (5.8)	−1.1 (5.7)	−1.0 (6.2)
TR aBMD	6.0 (5.7)	5.8 (5.6)	7.0 (7.3)	−1.6 (6.2)	−1.6 (6.1)	−1.2 (8.0)
TH aBMD	3.7 (4.2)	3.5 (4.2)	4.3 (4.8)	−1.6 (4.9)	−1.5 (4.8)	−1.7 (5.5)

The relative contributions of cortical versus trabecular bone to the transference of load has generally been related to their relative proportions in terms of mass [7, 9], so that the smaller proportion of trabecular bone mass in the osteoporotic femur equates to a smaller contribution to overall strength. However, reduction in vBMD by age is higher in trabecular than in cortical bone [26], and vBMD differences between hip fracture and control postmenopausal women are higher in trabecular than in cortical bone [5]. Cortical buckling has been suggested as a possible mechanism of hip fracture during sideways fall [1, 3, 27, 28], and trabecular

bone may play an important role in preventing cortical buckling since it provide about 40 % of the resistance to cortical buckling, and a small increase in subcortical trabecular bone results in a disproportionately large increase in cortical stability [3]. All these highlight the importance of trabecular bone in hip fracture aetiology. Anti-resorptive therapy consistently show that reduction in fracture risk is associated with improvement of trabecular vBMD [12–17], and this study confirms this, too.

We observed significant differences in baseline cortical and trabecular vBMD between this study and the previous

Table 5 Percentage change of volume at year 3 from baseline

	Zoledronic Acid (n=94)			Placebo (n=85)		
	Cortical	Trabecular	Integral	Cortical	Trabecular	Integral
Total FN	3.7 (13.4)	−0.4 (11.2)	0.8 (11.1)	1.5 (10.8)	−1.7 (9.4)	−0.8 (9.1)
Total TR	4.3 (7.0)	0.5 (4.9)	1.5 (4.7)	1.7 (6.0)	−0.1 (5.4)	0.4 (4.8)
TH	3.5 (8.3)	0.1 (8.4)	1.1 (8.4)	1.2 (8.2)	−0.5 (8.5)	0.0 (8.4)
Proximal FN	4.3 (13.7)	1.6 (12.2)	2.3 (12.9)	3.3 (10.7)	2.6 (9.8)	2.8 (10.2)
Middle FN	1.8 (18.6)	0.2 (17.1)	0.7 (17.9)	0.9 (17.8)	0.4 (17.2)	0.5 (17.5)
Distal FN	2.8 (16.2)	0.9 (15.7)	1.5 (16.0)	2.3 (12.7)	0.5 (12.8)	1.1 (12.8)
Middle TR	−0.1 (6.3)	−1.8 (8.3)	−1.4 (7.4)	−0.2 (5.8)	−1.6 (8.2)	−1.4 (7.1)
Distal TR	1.6 (5.4)	0.1 (9.0)	0.6 (7.4)	−0.5 (5.8)	−0.5 (7.3)	−0.5 (6.6)
Inferomedial FN	3.2 (13.0)	0.3 (10.7)	0.1 (8.4)	1.0 (12.5)	0.8 (9.1)	0.4 (7.7)
Anterior FN	6.2 (11.6)	3.5 (9.6)	3.4 (7.5)	4.9 (9.8)	2.9 (9.9)	3.2 (7.0)
Superolateral FN	3.1 (11.7)	0.5 (10.7)	0.1 (7.9)	2.6 (9.9)	0.3 (10.0)	0.4 (7.0)
Posterior FN	5.6 (11.2)	3.3 (10.0)	3.1 (7.5)	3.7 (8.9)	2.7 (8.8)	2.7 (6.2)

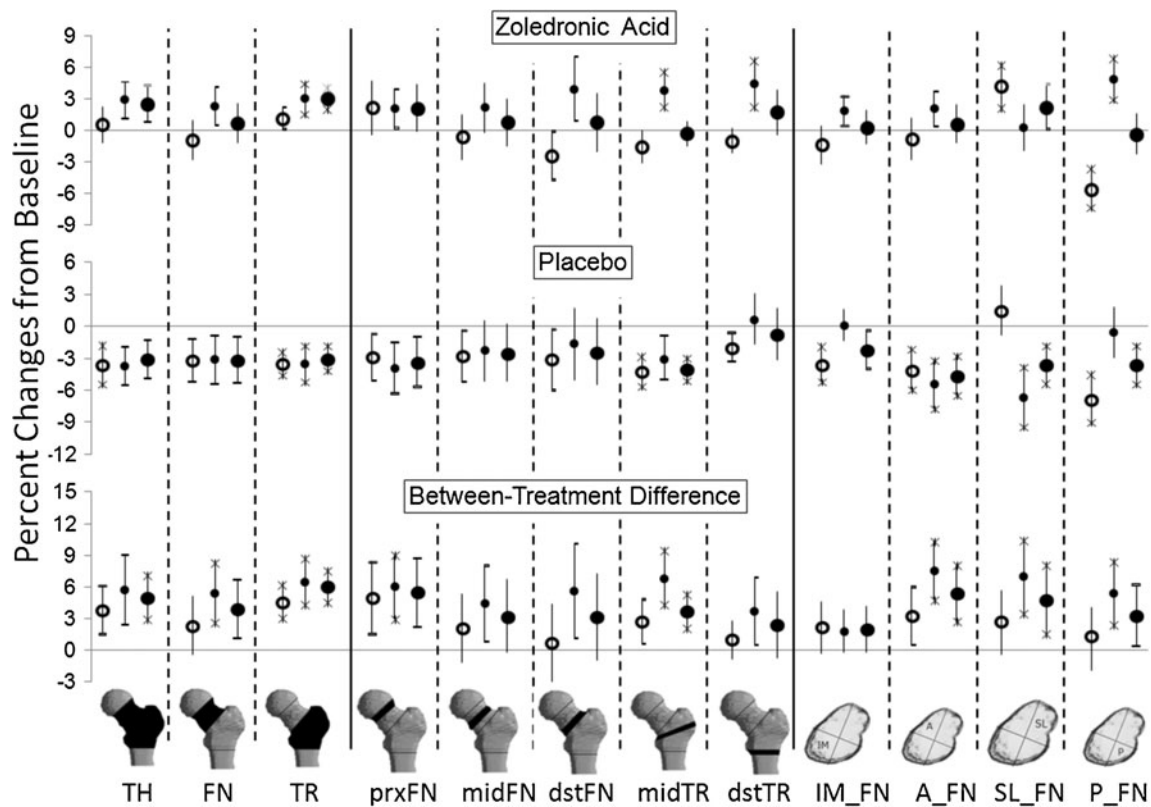


Fig. 3 Mean percentage changes in cortical (*open circle*), trabecular (*small solid circle*) and integral (*larger solid circle*) vBMD from baseline in the different partitions of the proximal femur. FN stands for the femoral neck, TR for trochanter, TH for total hip, *prx* for proximal, *mid* for middle, *dst* for distal, IM for inferomedial quadrant, A

for anterior, P for posterior and SL for superolateral. The *error bars* represent 95 % CI and the *end caps hyphen, horizontal bar and asterisk* indicate the mean significantly different from zero at $p < 0.05$, $p < 0.01$ and $p < 0.001$, respectively

analysis [14], whereas the integral TR and FN vBMDs were similar. This is most likely due to the use of different softwares for the analysis, and differences in the way in which the cortical and trabecular regions were defined since patient characteristics and aBMD of this analysis are similar to the previous analysis and the whole HORIZON PFT (Table 1). We defined cortical bone using a method based on the evaluation of density profiles perpendicular to the periosteal bone surface [10, 19] and defined trabecular bone as the total bone minus the cortical bone. The earlier analysis defined the trabecular region by uniform erosion of the periosteal bone surface, so that it was completely within the medullary volume [29, 30] and applied a threshold of 350 mg/cm^3 to define cortical bone in the cortical region (between periosteal surface and trabecular region). As a consequence, the trabecular volume as defined by our method was larger, and it included subcortical trabecular bone situated immediately adjacent to endocortical bone, which is much denser than the more central trabecular bone. This was evidenced by a much higher baseline trabecular vBMD in this study ($96\text{--}143 \text{ mg/cm}^3$ at the FN, TR and TH) compared with the previous analysis ($22\text{--}66 \text{ mg/cm}^3$). A

significantly ($p < 0.05$) lower cortical vBMD was also seen in this study compared with the previous study ($397\text{--}431$ v. $453\text{--}476 \text{ mg/cm}^3$ at the FN, TR and TH), reflecting the effects of using a cortical threshold of 350 mg/cm^3 in the previous study.

Like the previous analysis [14], we found significant decrease from baseline of cortical, trabecular and integral vBMDs at the FN, TR and TH of the placebo group and significant percentage increase from baseline of TH integral vBMD in the zoledronic acid group. We observed between-treatment effect on FN trabecular vBMD, whereas the previous analysis did not. We also observed lower increases in trabecular vBMD at the TR and TH in response to zoledronic acid than were reported in an earlier analysis (around 6–7 % compared to 11 %). Differences in image analysis methods again may be the cause. Much lower trabecular vBMD was found in the previous analysis, and for a given change in trabecular vBMD, the percentage change would be larger if the baseline vBMD was lower. Another possible reason for the discrepancy is that we analysed 179 patients with both baseline and 36-month scans, whereas the previous study analysed 232 baseline and 179 follow-up scans.

This study has some limitations. Although our study sample was representative for the QCT and HORIZON PFT cohorts in terms of baseline patient characteristics and aBMD (Tables 1 and 4), it was limited to patients with both baseline and 36-month QCT scans and did not include 54 patients with baseline QCT only, this may reduce the study power. Our sample size was appropriate for the investigation of between-treatment differences in bone macrostructure, which was the aim of this study, but a larger study population would be required to directly test the effects of these differences on the incidence of hip fracture. There is an inherent limitation to the accuracy of cortical vBMD measurement using QCT, particularly at the superolateral aspect of the FN where the cortex is thin. The QCT scan with 0.97×0.97 -mm in-plane pixel size and 3-mm slice thickness provides limited details of the thin cortex and curvatures at the FN and TR and does not provide information about trabecular microstructure, submillimetre changes in geometry, the rate of bone remodelling (stress raisers) or bone micro-damage. Recent advances in QCT technology with high-resolution CT may have produced the capacity to detect microstructural treatment effects within 12 months for vertebra [31]. We ignored the femoral head in the QCT analysis, whereas a recent study demonstrated that trabecular vBMD deficit between postmenopausal women with and without hip fracture was 38 % higher at the femoral head than at the FN [5].

In conclusion, an annual infusion of 5 mg of zoledronic acid for a period of 3 years resulted in site-specific differential increases in vBMD, particularly in trabecular compartment and in regions known to be associated with the initiation of hip fracture.

Acknowledgments We would like to thank our sponsors, the Medical Research Council and the National Institute for Health Research (NIHR). The HORIZON PFT was sponsored by Novartis Pharma AG, Basel, Switzerland. The views expressed in this publication are those of the author(s) and not necessarily those of the NHS, the NIHR or the Department of Health. Acknowledgements go to the editorial board of the Sheffield NIHR Bone Biomedical Research Unit for their help in preparing this manuscript.

Conflicts of interest Dr. Eastell serves as a consultant, has received honoraria for speaking, and has received grant funding from Novartis, Amgen, Sanofi-Aventis, Lilly, Organon, Pfizer, and Procter & Gamble Pharmaceuticals. Dr. Black serves as a consultant for Nycomed and Zosano and has research contracts with Novartis and Roche. Other authors have no conflict of interest.

References

1. Mayhew PM, Thomas CD, Clement JG, Loveridge N, Beck TJ, Bonfield W, Burgoyne CJ, Reeve J (2005) Relation between age, femoral neck cortical stability, and hip fracture risk. *Lancet* 366:129–135
2. Poole KE, Mayhew PM, Rose CM, Brown JK, Bearcroft PJ, Loveridge N, Reeve J (2009) Changing structure of the femoral neck across the adult female lifespan. *J Bone Miner Res* 25:482–491
3. Thomas CD, Mayhew PM, Power J, Poole KE, Loveridge N, Clement JG, Burgoyne CJ, Reeve J (2009) Femoral neck trabecular bone: loss with ageing and role in preventing fracture. *J Bone Miner Res* 24(11):1808–1818
4. de Bakker PM, Manske SL, Ebacher V, Oxland TR, Crompton PA, Guy P (2009) During sideways falls proximal femur fractures initiate in the superolateral cortex: evidence from high-speed video of simulated fractures. *J Biomech* 42:1917–1925
5. Bousson VD, Adams J, Engelke K, Aout M, Cohen-Solal M, Bergot C, Haguenaer D, Goldberg D, Champion K, Aksouh R, Vicaud E, Laredo JD (2011) In vivo discrimination of hip fracture with quantitative computed tomography: results from the prospective European Femur Fracture Study (EFFECT). *J Bone Miner Res* 26:881–893
6. Boussein ML, Fajardo RJ (2005) Cortical stability of the femoral neck and hip fracture risk. *Lancet* 366:1523–1524
7. Lotz JC, Cheal EJ, Hayes WC (1995) Stress distributions within the proximal femur during gait and falls: implications for osteoporotic fracture. *Osteoporos Int* 5:252–261
8. Werner C, Iversen BF, Therkildsen MH (1988) Contribution of the trabecular component to mechanical strength and bone mineral content of the femoral neck. An experimental study on cadaver bones. *Scand J Clin Lab Invest* 48:457–460
9. Verhulp E, Van RB, Huiskes R (2008) Load distribution in the healthy and osteoporotic human proximal femur during a fall to the side. *Bone* 42:30–35
10. Yang L, Maric I, McCloskey EV, Eastell R (2008) Shape, structural properties and cortical stability along the femoral neck: a study using clinical QCT. *J Clin Densitom* 11:373–382
11. Crabtree N, Loveridge N, Parker M, Rushton N, Power J, Bell KL, Beck TJ, Reeve J (2001) Intracapsular hip fracture and the region-specific loss of cortical bone: analysis by peripheral quantitative computed tomography. *J Bone Miner Res* 16:1318–1328
12. Black DM, Greenspan SL, Ensrud KE, Palermo L, McGowan JA, Lang TF, Garner P, Boussein ML, Bilezikian JP, Rosen CJ (2003) The effects of parathyroid hormone and alendronate alone or in combination in postmenopausal osteoporosis. *N Engl J Med* 349:1207–1215
13. Black DM, Bilezikian JP, Ensrud KE, Greenspan SL, Palermo L, Hue T, Lang TF, McGowan JA, Rosen CJ (2005) One year of alendronate after one year of parathyroid hormone (1–84) for osteoporosis. *N Engl J Med* 353:555–565
14. Eastell R, Lang T, Boonen S, Cummings S, Delmas PD, Cauley JA, Horowitz Z, Kerzberg E, Bianchi G, Kendler D, Leung P, Man Z, Mesenbrink P, Eriksen EF, Black DM (2010) Effect of once-yearly zoledronic acid on the spine and hip as measured by quantitative computed tomography: results of the HORIZON Pivotal Fracture Trial. *Osteoporos Int* 21:1277–1285
15. Genant HK, Lang T, Fuerst T, Pinette KV, Zhou C, Thiebaud D, ez-Perez A (2004) Treatment with raloxifene for 2 years increases vertebral bone mineral density as measured by volumetric quantitative computed tomography. *Bone* 35:1164–1168
16. Lewiecki EM, Keaveny TM, Kopperdahl DL, Genant HK, Engelke K, Fuerst T, Kivitz A, Davies RY, Fitzpatrick LA (2009) Once-monthly oral ibandronate improves biomechanical determinants of bone strength in women with postmenopausal osteoporosis. *J Clin Endocrinol Metab* 94:171–180
17. McClung MR, Zanchetta JR, Hoiseth A, Kendler DL, Yuen CK, Brown JP, Stonkus S, Goemaere S, Recknor C, Woodson GC, Bolognese MA, Franek E, Brandi ML, Wang A, Libanati C

- (2012) Denosumab Densitometric changes assessed by quantitative computed tomography at the spine and hip in postmenopausal women with osteoporosis. *J Clin Densitom* 15(2):176–185
18. Poole KE, Treece GM, Ridgway GR, Mayhew PM, Borggreffe J, Gee AH (2011) Targeted regeneration of bone in the osteoporotic human femur. *PLoS One* 6:e16190
 19. Yang L, Prevrhal S, McCloskey EV, Eastell R (2008) A method to estimate femoral neck cortical thickness from clinical QCT scans. *Calcif Tissue Int* 82:S181–S182
 20. Hangartner TN, Gilsanz V (1996) Evaluation of cortical bone by computed tomography. *J Bone Miner Res* 11:1518–1525
 21. Prevrhal S, Fox JC, Shepherd JA, Genant HK (2003) Accuracy of CT-based thickness measurement of thin structures: modeling of limited spatial resolution in all three dimensions. *Med Phys* 30:1–8
 22. Black DM, Delmas PD, Eastell R, Reid IR, Boonen S, Cauley JA, Cosman F, Lakatos P, Leung PC, Man Z, Mautalen C, Mesenbrink P, Hu H, Caminis J, Tong K, Rosario-Jansen T, Krasnow J, Hue TF, Sellmeyer D, Eriksen EF, Cummings SR (2007) Once-yearly zoledronic acid for treatment of postmenopausal osteoporosis. *N Engl J Med* 356:1809–1822
 23. Bell KL, Loveridge N, Power J, Garrahan N, Stanton M, Lunt M, Meggitt BF, Reeve J (1999) Structure of the femoral neck in hip fracture: cortical bone loss in the inferoanterior to superoposterior axis. *J Bone Miner Res* 14:111–119
 24. Bell KL, Loveridge N, Power J, Rushton N, Reeve J (1999) Intra-capsular hip fracture: increased cortical remodeling in the thinned and porous anterior region of the femoral neck. *Osteoporos Int* 10:248–257
 25. Crabtree NJ, Kroger H, Martin A, Pols HA, Lorenc R, Nijs J, Stepan JJ, Falch JA, Miazgowski T, Grazio S, Raptou P, Adams J, Collings A, Khaw KT, Rushton N, Lunt M, Dixon AK, Reeve J (2002) Improving risk assessment: hip geometry, bone mineral distribution and bone strength in hip fracture cases and controls. The EPOS study. European Prospective Osteoporosis Study. *Osteoporos Int* 13:48–54
 26. Riggs BL, Melton IL III, Robb RA, Camp JJ, Atkinson EJ, Peterson JM, Rouleau PA, McCollough CH, Bouxsein ML, Khosla S (2004) Population-based study of age and sex differences in bone volumetric density, size, geometry, and structure at different skeletal sites. *J Bone Miner Res* 19:1945–1954
 27. Kaptoge S, Beck TJ, Reeve J, Stone KL, Hillier TA, Cauley JA, Cummings SR (2008) Prediction of incident hip fracture risk by femur geometry variables measured by hip structural analysis in the study of osteoporotic fractures. *J Bone Miner Res* 23:1892–1904
 28. Rivadeneira F, Zillikens MC, de Laet CE, Hofman A, Uitterlinden AG, Beck TJ, Pols HA (2007) Femoral neck BMD is a strong predictor of hip fracture susceptibility in elderly men and women because it detects cortical bone instability: the Rotterdam Study. *J Bone Miner Res* 22:1782–1790
 29. Cheng X, Li J, Lu Y, Keyak J, Lang T (2007) Proximal femoral density and geometry measurements by quantitative computed tomography: association with hip fracture. *Bone* 40:169–174
 30. Lang T, LeBlanc A, Evans H, Lu Y, Genant HK, Yu A (2004) Cortical and trabecular bone mineral loss from the spine and hip in long-duration spaceflight. *J Bone Miner Res* 19:1006–1012
 31. Graeff C, Timm W, Nickelsen TN, Farrerons J, Marin F, Barker C, Gluer CC (2007) Monitoring teriparatide-associated changes in vertebral microstructure by high-resolution CT in vivo: results from the EUROFOR study. *J Bone Miner Res* 22:1426–1433